Organic & Biomolecular Chemistry

Dynamic Article Links

Cite this: *Org. Biomol. Chem.*, 2012, **10**, 869

www.rsc.org/obc

PAPER

Synthesis of *N*-(2-chloro purin-6-yl) aza-18-crown-6 and its interaction with human serum albumin

Cui Li,[b] Fengling Cui,*[a] Runze Mao,[a] Ruina Huo[a] and Guirong Qu[a]

Received 24th July 2011, Accepted 10th October 2011
DOI: 10.1039/c1ob06241g

The synthesis of novel purine nucleosides-linked azacrown ethers in the C6 position, *N*-(2-chloro purin-6-yl) aza-18-crown-6 (NCPAC), was described. This new nucleoside analogue can be prepared from a series of N9-modified nucleosides and the method allows for new and easy modification of the nucleosides. The interaction between NCPAC and human serum albumin (HSA) was studied using molecular docking and fluorescence techniques. Thermodynamics revealed that the interaction was entropy driven with predominantly hydrophobic forces. From the observed Föster's-type fluorescence resonance energy transfer, the donor (Trp 214 in HSA) to acceptor (NCPAC) distance was calculated to be 3.6 nm. The conformational changes of HSA due to the interaction were investigated qualitatively from synchronous fluorescence spectra. Molecular docking studies were performed to obtain information on the possible residues involved in the interaction process.

Introduction

Many nucleoside analogues with modifications on the heterocyclic bases have been investigated for their antiviral and anticancer activities. Purine derivatives with various substituents at C6 received considerable attention due to their important physiological and pharmacological properties.[1] C6-aminopurines were shown to have antitumor activity as kinase inhibitors.[2]

Crown ethers, first introduced in 1967 by Pedersen, are probably one of the most intriguing class of compounds in the field of supramolecular chemistry.[3] Owing to the high selectivity for alkali metal and primary ammonium cations,[4] crown ethers as suitable receptors were attached to fluorescence as a method for the selective detection of metal cations, which play an important role in biological studies.[5]

Based on our preliminary study on the various modifications of nucleoside analogues, we synthesized a series of purine analogues-linked azacrown ethers at the C6 position.[6] In this work, we designed and prepared novel purine nucleosides C6-modified by azacrown ethers, *N*-(2-chloro purin-6-yl) aza-18-crown-6 (NCPAC) (Fig. 1), aiming at providing an efficient route to new nucleoside analogues, which could be applied to develop biologically active compounds.

Human serum albumin (HSA) consists of a single polypeptide chain of 585 amino acid residues and is the most abundant carrier protein in blood plasma.[7] It considerably contributes to colloid osmotic pressure and has important physiological functions, which are to store and transport a variety of endogenous and exogenous compounds, such as hormones, fatty acids, amino acids, cations, anions and numerous drugs.[8] Many are orally active drugs that have been developed by the pharmaceutical industry bind to protein targets.[9] It was shown that the distribution, free concentration and the metabolism of various drugs could be significantly altered as a result of their binding to HSA.[10] Drug interactions with proteins would, in most cases, significantly affect the elimination rate of the drug. Extensive investigations on interactions between proteins and components of living systems or pharmaceutical molecules were carried out,[11,12] because such studies could provide information on the features which could affect the therapeutic effect of drugs. In this work, the interaction between NCPAC and human serum albumin (HSA) was studied using molecular docking and fluorescence techniques for the first time. The study can help us better understand the binding mode and binding mechanism between nucleoside analogues and HSA. And then it would be of great significance for the design and synthesis of new nucleosides that have the maximum effectiveness.

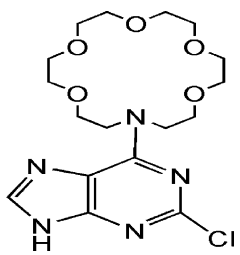

Fig. 1 The molecular structure of *N*-(2-chloro purin-6-yl)aza-18-crown-6 (NCPAC).

[a]*College of Chemistry and Environmental Science, Henan Normal University, Xinxiang, 453007, China. E-mail: fenglingcui@hotmail.com*
[b]*School of Automation & Electrical Engineering, University of Science and Technology Beijing, Beijing, 100083, China*

Experimental

The preparation of NCPAC

Crown ethers bearing nucleosides 3 *via* the alkylation of **1** with (poly)ethylene glycol ditosylate **2** were synthesized in THF in the presence of sodium hydride (Scheme 1). Crown ether **3** was purified by column chromatography in yields of 38%, then its structure was confirmed by NMR spectra (Fig. 2) and high-resolution mass spectrometry.

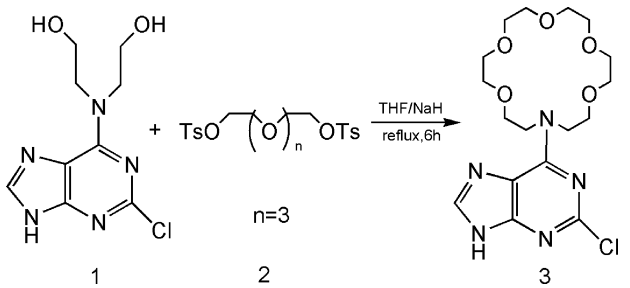

Scheme 1 The reaction of (poly)ethylene glycol ditosylates with 6-bis (2-hydroxyethyl) aminopurines.

NCPAC: White powder, mp 130–132 °C ^{1}H NMR ($CDCl_3$, 400 MHz) δ 13.18 (s, 1H), 8.14 (s, 1H), 4.40 (s, 2H), 3.86 (d, J = 5.2 Hz, 2H), 3.68 (t, J = 6.8 Hz, 2H), 3.55 (s, 16H). ^{13}C NMR ($CDCl_3$, 100 MHz) δ 155.9, 153.9, 140.4, 119.3, 72.5, 72.2, 72.0, 71.2, 70.8, 70.2, 51.5, 50.3. HRMS: calcd for $C_{22}H_{29}N_5O_4$ [M + Na^+] 438.1520, found 438.1519.

Materials

HSA was purchased from Sigma. The stock solutions of 2.0×10^{-5} mol L^{-1} HSA and 1.0×10^{-3} mol L^{-1} NCPAC were prepared by directly dissolving raw materials into double distilled water and kept in the dark at 0–4 °C. All other reagents were of analytical grade. Double distilled water was used throughout the experiment.

Apparatus and methods

All fluorescence measurements were carried out by using a FP-6500 spectrofluorimeter (JASCO, Japan). A T6 UV-vis spectrophotometer (Beijing Purkinje General Instrument Co. Ltd.,

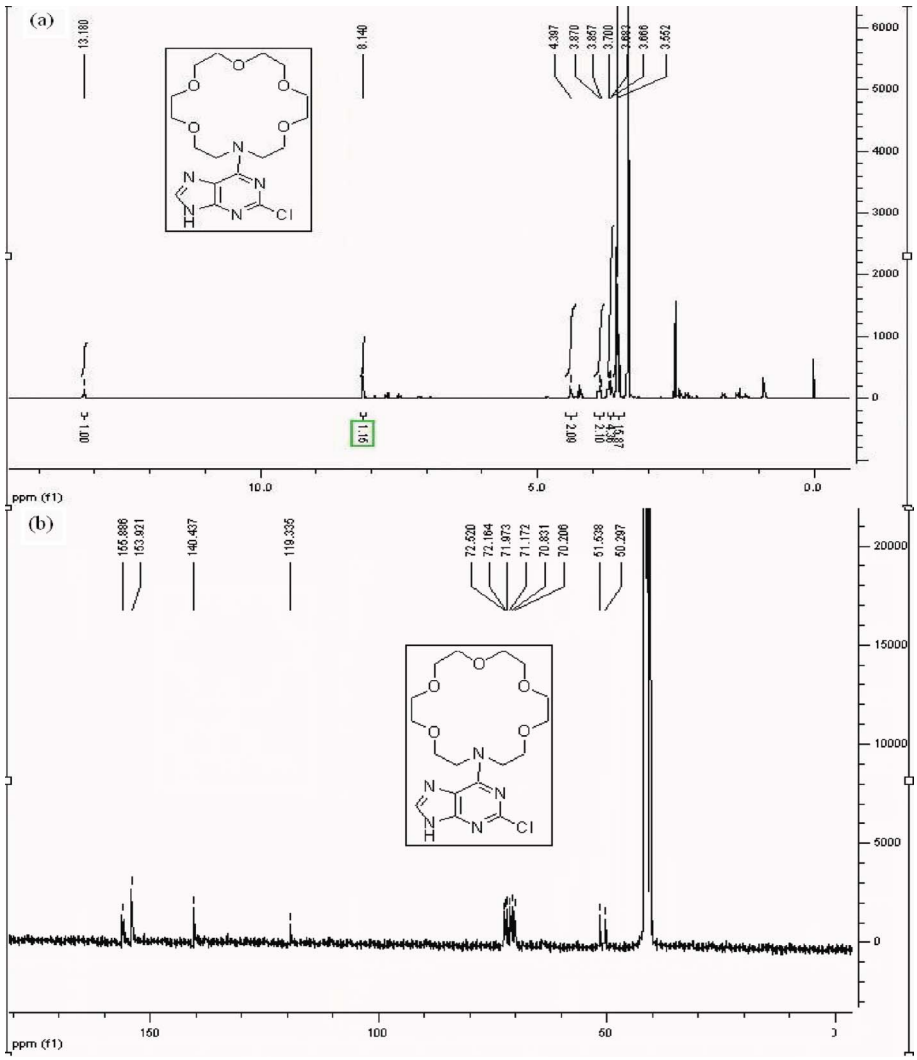

Fig. 2 The ^{1}H NMR (a) and ^{13}C NMR (b) of NCPAC.

China) was applied to measure UV absorption spectra. pH values were measured by a pH-3digital pH-meter (Shanghai Lei Ci Device Works, Shanghai, China) with a combined glass electrode. All calculations of the molecular docking were performed on a SGI workstation.

Fluorescence measurements. 2.0 mL Tris-HCl buffer solution, 2.0 mL NaCl solution, appropriate amount of NCPAC and HSA were added to a 10 mL standard flask, and then diluted to 10 mL with double distilled water. Fluorescence quenching spectra of HSA were measured at excitation and emission wavelengths of $\lambda_{ex} = 282$ nm and $\lambda_{em} = 290$–450 nm, respectively. The synchronous fluorescence spectra were recorded from 280–340 nm at $\Delta\lambda = 15$ nm and 310–380 nm at $\Delta\lambda = 60$ nm, respectively.

Molecular docking study. The docking study of the binding mode between NCPAC and HSA was performed on SGI FUEL workstation. The 3D structure of HSA in complex with myristic acid and the *R*-(+) enantiomer of warfarin was downloaded from the Brookhaven Protein Data Bank (PDB entry code: 1H9Z). The initial structure of NCPAC was sketched by molecular docking software Sybyl 6.9.2. The geometry was subsequently optimized using the Tripos force field with Gasteiger–Huckel charges. The co-crystalled ligand and water molecules from the crystal structure were removed and hydrogen atoms were added. The FlexX module in Sybyl 6.9.1 [13] was used to calculate the interaction mode between drug and HSA. During the docking process, a maximum of 30 conformers were considered for this compound. The conformer with the lowest binding free energy was used for further analysis.

Results and Discussion

Fluorescence quenching study

Fluorescence quenching of proteins provides information about ligand binding to specific sites.[14] In collisional quenching, the fluorophore and quencher come into contact during the lifetime of the excited state, whereas static quenching generally forms a fluorophore–quencher complex. When small molecules bind to HSA, changes of intrinsic fluorescence intensity of HSA are induced by the microenvironment of tryptophan residues. The fluorescence emission spectra of HSA at different concentrations of NCPAC are shown in Fig. 3. It can be seen that HSA had a strong fluorescence emission band at 340 nm at an excitation wavelength of 282 nm, while NCPAC had no intrinsic fluorescence under the present experimental conditions. The fluorescence intensity of HSA decreased regularly from 92 to 52 while the concentration of NCPAC increased. The strong quenching of HSA fluorescence and a small blue shift might suggest that NCPAC interacted with HSA, the microenvironment of tryptophan residues was altered, the hydrophobicity enhanced, and the conformation of HSA might be changed.[15,16]

Quenching mechanisms

The dynamic quenching and static quenching could be differentiated by comparing the quenching rate constants at different temperatures. The quenching rate constants decrease with increasing temperature for static quenching, but a reverse effect is observed for dynamic quenching.[17] The possible quenching mechanisms could be investigated by the fluorescence quenching

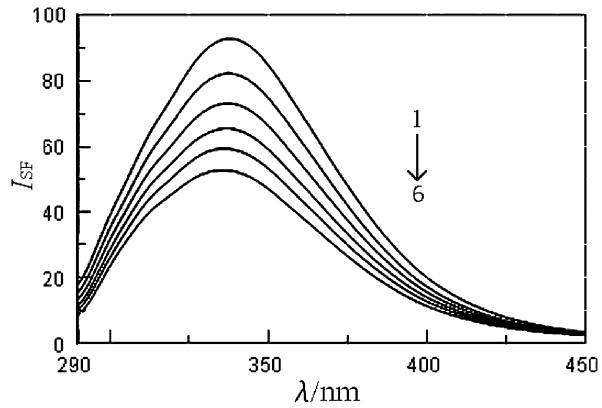

Fig. 3 The fluorescence emission spectra of HSA at various concentrations of NCPAC. $C_{HSA} = 4.0 \times 10^{-7}$ mol L^{-1}; from 1 to 6: $C_{NCPAC} = 0$, 0.1, 0.2, 0.3, 0.4, 0.5×10^{-6} mol L^{-1}.

spectra of HSA. The Stern–Volmer curves of NCPAC with HSA at different temperatures (293, 303 and 313 K) are shown in Fig. 4. The Stern–Volmer plots were linear and the slopes decrease with increasing temperature, indicating that the interaction between NCPAC and HSA was a static quenching. In order to confirm this point, the procedure was assumed to be dynamic quenching. The fluorescence quenching data were analyzed by the Stern–Volmer equation,[18]

$$F_0/F = 1 + K_q \tau_0 [Q] = 1 + K_{sv}[Q] \quad (1)$$

where F and F_0 are the fluorescence intensities with and without quenchers, respectively. K_q is the quenching rate constants of the molecule, K_{sv} is the Stern–Volmer quenching constant, τ_0 is the average lifetime of fluorescence molecule without quencher and $[Q]$ is the concentration of quencher. Obviously,

$$K_{sv} = K_q \tau_0 \quad (2)$$

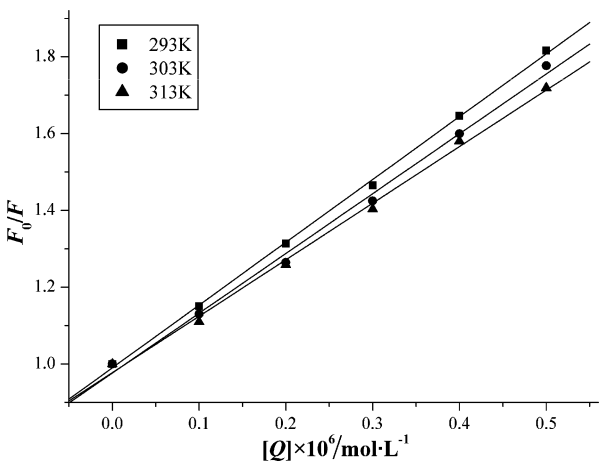

Fig. 4 The Stern–Volmer curves for NCPAC quenching the fluorescence of HSA.

The τ_0 of HSA is 10^{-8} s,[19] so the K_q could be obtained according to eqn (2). The results are listed in Table 1 together with correlation coefficients.

The limiting diffusion constant of the biomolecule K_{dif} is 2.0×10^{10} L mol^{-1} s^{-1}.[20] Obviously, the quenching rate constants K_q

Table 1 The quenching constants between HSA and NCPAC by Stern–Volmer equation

T/K	Stern–Volmer equation	K_q (L mol^{-1} S^{-1})	R
293	$Y = 0.9901 + 7.355 \times 10^6[Q]$	7.355×10^{14}	0.9995
303	$Y = 0.9724 + 7.010 \times 10^6[Q]$	7.010×10^{14}	0.9998
313	$Y = 0.9772 + 6.624 \times 10^6[Q]$	6.624×10^{14}	0.9981

was larger than K_{dif}. As a result, the quenching was not dynamic quenching but results from formation of a complex.

Binding sites

In drug-protein binding studies, the Scatchard eqn (3) is frequently used for binding constant calculation:[21]

$$r/D_f = nK - rK \quad (3)$$

where r is the number of moles of drug bound per mole of protein, D_f is the concentration of free drug, K is the binding constant, and n is the number of binding sites. The Scatchard plots for the NCPAC–HSA system at different temperatures are shown in Fig. 5. The values of K and n were listed in Table 2. The linearity of the Scatchard plots indicated that NCPAC bound to a single class of binding sites on HSA, which was consistent with the number of binding sites n. It could be seen that there was a strong interaction between NCPAC and HSA through the value of K in Table 2. The K decreased while the temperature increased, resulting in a decrease in the stability of the NCPAC–HSA complex, but the effect of temperature was very small. Therefore, the quenching efficiency of NCPAC to HSA was obviously not diminished when the difference in temperature was not large.

Because the binding site is approximately 1, the binding constants obtained by using the static quenching equation, Lineweaver–Burk equation.

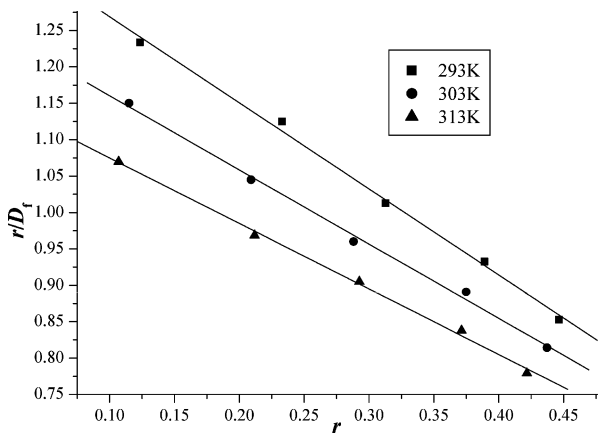

Fig. 5 The Scatchard curves for NCPAC quenching the fluorescence of HSA.

Table 2 The binding constants and binding sites of the interaction between NCPAC and HSA by Scatchard equation

T/K	Scatchard equation	K (L mol^{-1})	n	R
293	$Y = 1.387 \times 10^5 - 1.182 \times 10^5 r$	1.182×10^5	1.173	0.9983
303	$Y = 1.262 \times 10^5 - 1.019 \times 10^5 r$	1.019×10^5	1.238	0.9982
313	$Y = 1.165 \times 10^5 - 0.8999 \times 10^5 r$	0.8999×10^5	1.294	0.9987

Table 3 The binding constants between HSA and NCPAC by Lineweaver–Burk equation

T/K	Lineweaver–Burk equation	K (L mol^{-1})	R
293	$Y = 0.716 \times 10^{-2} + 0.3249 \times 10^{-7} 1/[Q]$	2.204×10^5	0.9997
303	$Y = 0.792 \times 10^{-2} + 0.3897 \times 10^{-7} 1/[Q]$	2.032×10^5	0.9997
313	$Y = 0.576 \times 10^{-2} + 0.4550 \times 10^{-7} 1/[Q]$	1.266×10^5	0.9993

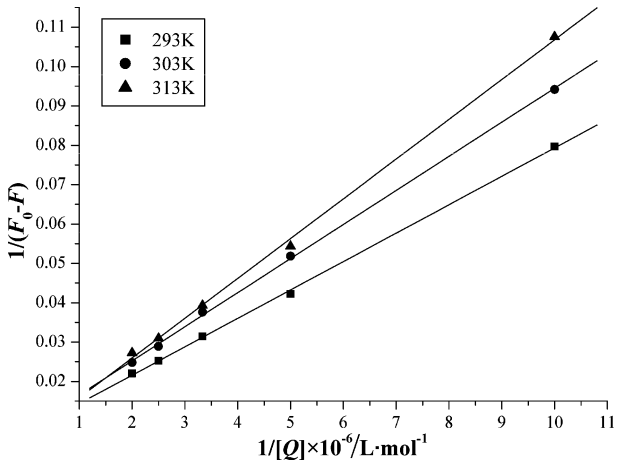

Fig. 6 The Lineweaver–Burk curves for NCPAC quenching the fluorescence of HSA at pH 7.40.

$$(F_0 - F)^{-1} = F_0^{-1} + K^{-1}F_0^{-1}[Q]^{-1} \quad (4)$$

where K is the binding constant of the drug with HSA, which can be calculated from the slope and intercept of the Lineweaver–Burk (Fig. 6), K = intercept/slope. The results are listed in Table 3.

Above all, the binding between NCPAC and HSA was remarkable and the effect of temperature was not significant. Due to the above findings, NCPAC was able to be stored and removed by HSA in the body.

Binding mode

Generally, small molecules are bound to macromolecules through four binding modes: hydrogen bond, van der Waals force, electrostatic and hydrophobic interactions.[22]

The thermodynamic parameters, enthalpy change (ΔH) and entropy change (ΔS) of reaction are important for confirming the acting force. For this reason, the temperature dependence of the binding constant was studied at 293, 303, and 313 K. The thermodynamic parameters could be determined from the van't Hoff equation,

$$\ln K = -\Delta H/RT + \Delta S/R \quad (5)$$

K is the binding constant at temperature T and R is gas constant. The values of ΔH and ΔS were obtained from linear van't Hoff plot (Fig. 7) and presented in Table 4. The value of ΔG was calculated from the equation,

$$\Delta G = \Delta H - T\Delta S = -RT\ln K \quad (6)$$

It was reported the characteristic sign of the thermodynamic parameter associated with the various individual kinds of interaction that may take place in the protein association process.[23,24] From the point of view of water structure, a positive ΔS value is frequently taken as evidence for hydrophobic interaction. Moreover, specific

Table 4 Thermodynamic parameters of NCPAC–HSA interaction at pH 7.4

Complex	T/K	ΔG (kJ mol^{-1})	ΔH (kJ mol^{-1})	ΔS (J mol^{-1} K^{-1})
NCPAC–HSA	293	−28.45	−10.87	60.0
	303	−29.05		
	313	−29.69		

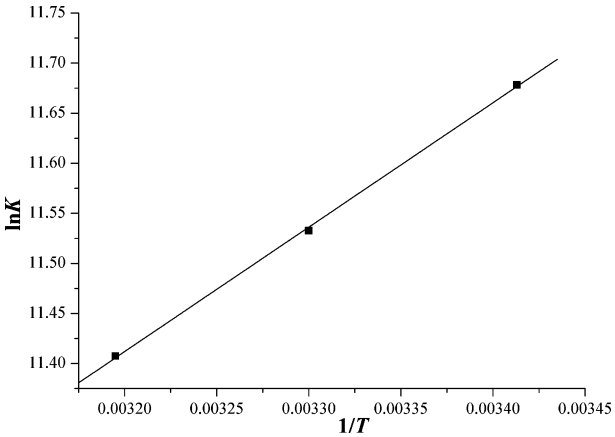

Fig. 7 The van't Hoff plot for the interaction of NCPAC and HSA.

electrostatic interactions between ionic species in aqueous solution are characterized by a positive ΔS value and a negative ΔH value. As shown in Table 4, ΔS was a positive value and ΔH was a negative value. Accordingly, it was not possible to account for the thermodynamic parameters of the NCPAC–HSA complex on the basis of a single intermolecular force model. It was more likely that hydrophobic, electrostatic interactions were involved in its binding process.

Binding distance

According to the Förster's non-radiative energy transfer theory,[25] the rate of energy transfer depends on: (i) the relative orientation of the donor and acceptor dipoles; (ii) the extent of the spectra overlap region between the donor emission spectrum and the acceptor absorption spectrum; (iii) the distance between the donor and the acceptor; (iv) the critical energy transfer distance. (iii) and (iv) can be simplified expressed into the following equation,

$$E = R_0^6/(R_0^6 + r^6) \quad (7)$$

where r is the distance between the acceptor and the donor and R_0 is the critical distance when the transfer efficiency is 50%, which could be calculated by eqn (8),

$$R_0^6 = 8.8 \times 10^{-25} k^2 N^{-4} \phi J \quad (8)$$

where k^2 is the spatial orientation factor between the emission dipole of the donor and the absorption dipole of the acceptor, N is the refractive index of the medium, ϕ is the fluorescence quantum yield of the donor, J is the overlap integral of the fluorescence emission spectrum of the donor and the absorption spectrum of the acceptor. The dipole orientation factor k^2 is the least certain parameter in calculation of the R_0. Although k^2 can range from 0 to 4 in theory, the extreme values require very rigid orientations. If both the donor and acceptor are tumbling rapidly and free to assume any orientation, then k^2 equals 2/3.[26] If only the donor is free to rotate, then k^2 can vary from 1/3 to 4/3.[27,28] The value of J could be given by eqn (9),

$$J = \Sigma F(\lambda)\varepsilon(\lambda)\lambda^4 \Delta\lambda / \Sigma F(\lambda)\Delta\lambda \quad (9)$$

where $F(\lambda)$ is the fluorescence intensity of the fluorescent donor at wavelength (λ) and is dimensionless, $\varepsilon(\lambda)$ is the molar absorption coefficient of the acceptor in wavelength (λ). The energy transfer efficiency is frequently calculated from the relative fluorescence yield in the presence (F) and absence (F_0) of acceptor,

$$E = 1 - F/F_0 \quad (10)$$

J could be evaluated by integrating the spectra in Fig. 8. It was reported for HSA that $k^2 = 2/3$, $\phi = 0.118$ and $N = 1.336$.[29] The value of J calculated from Fig. 8 was 0.99×10^{-14} cm^3 L mol^{-1}. Based on these data, the distance between NCPAC and the tryptophan residue in HSA, r was calculated to be 3.6 nm, a value smaller than 7 nm, confirming the static quenching interaction between NCPAC and HSA.

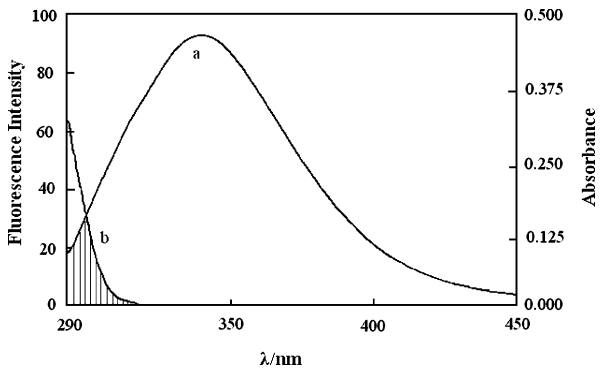

Fig. 8 The overlap of the fluorescence emission spectra of HSA (a) and UV absorption spectra of NCPAC (b). $C_{HSA} = 0.8 \times 10^{-6}$ mol L^{-1}; $C_{NCPAC} = 0.2 \times 10^{-5}$ mol L^{-1}.

Molecular docking

The complementary application of molecular docking by computer methods was employed to improve the understanding of the interaction between NCPAC and HSA. Descriptions of 3D structure of crystalline albumin revealed that HSA comprises of three homologous domains (I–III): I (residues 1–195), II (196–383), III (384–585), each domain is a product of subdomains that posses common structural motifs. The principal regions of ligand binding to HSA are located in hydrophobic cavities in subdomains IIA and IIIA, which are consistent with sites I and II, respectively. One tryptophan residue (Trp214) of HSA is in subdomain IIA.[30] Based on the approach of the molecular docking study, which is mentioned above, a computational model of the target receptor was built, which was used to calculate the partial binding parameters of the NCPAC–HSA system through SGI FUEL workstations. The best energy ranked results are shown in Fig. 9. The bisindolylmaleimide moiety was located within the binding pocket, and both rings were practically coplanar. It was noteworthy that the tryptophan residue (Trp214) and the lysine residue (Lys195) of HSA were in close proximity to the pentenyl moiety of NCPAC, suggesting the existence of a hydrophobic

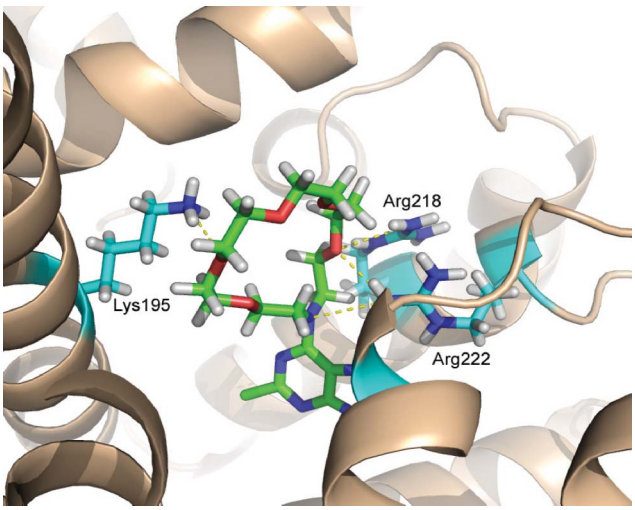

Fig. 9 A stereoview of the docked conformation of NCPAC in HSA.

interaction between them. Furthermore, this finding provided a good structural basis to explain the efficient fluorescence quenching of HSA emission in the presence of NCPAC. There were also hydrogen bonds between the drug and the polar amino acid residues: Arg 222 3.168 Å, Arg 218 3.192 Å, Lys 195 3.121 Å, from the IIA subdomain were able to form an intermolecular H-bond with the ring. On the other hand, the amino acid residues with a benzene ring matched the structure of NCPAC in space to firm the conformation of the complex. The ligand binding regions of HSA located in hydrophobic cavities in subdomains IIA were too large to accommodate the NCPAC. The calculated binding Gibbs free energy (ΔG) was –20.60 kJ mol^{-1}, which was close to the experimental data (–28.45 kJ mol^{-1}) in some degree. However, the results obtained from docking indicated that the interaction between NCPAC and HSA was dominated by hydrophobic force.

Conformation investigation

Synchronous fluorescence spectra are frequently used to characterize the interaction between molecular probes and proteins since it can provide information about the molecular microenvironment in the vicinity of the chromosphere molecules.[31] According to Miller,[32] the synchronous fluorescence spectra of HSA were obtained to consider the wavelength intervals $\Delta\lambda$ = 15 nm and $\Delta\lambda$ = 60 nm to evidence the characteristic of tyrosine and tryptophan residues, respectively.[33] Synchronous fluorescence spectra of HSA with various concentrations of NCPAC for $\Delta\lambda$ = 15 (a) and 60 nm (b) are shown in Fig. 10. Addition of the drug led to a dramatic decrease in the synchronous fluorescence intensity with a distinct shift of spectral peak from 299 to 301 nm (Fig. 10a) and 339 to 341 nm (Fig. 10b), respectively. It is considered that the maximum emission wavelength (λ_{max}) of the tryptophan residues is related to the polarity of the microenvironment. λ_{max} at 330–332 nm suggests that tryptophan residues are located in the non-polar region, that is, they are buried in a hydrophobic cavity of HSA; λ_{max} at 350–352 nm indicates that tryptophan residues are exposed to water, that is to say, the hydrophobic cavity in HSA is disaggregated and the structure of HSA is looser. In Fig. 10a, the fluorescence of tyrosine residues was quenched by NCPAC with a slight red shift. It was suggested that the polarity around the tyrosine residue increased. Fig. 10b shows distinctly that NCPAC mainly bound to the hydrophobic cavity of HSA, which was in agreement with the results from molecular docking and the thermodynamic parameters. It was also indicated that the polarity around the tryptophan residues was increased and the hydrophobicity was decreased. These indicated that the structure of HSA was changed.

The effects of other ions on the binding constants

The HSA molecule contains elements such as S, P, Cu, and Mn. In addition, some trace metal ions exist *in vivo*, which have a definite ability to bind to proteins.[34,35] In order to investigate the effect of coexisting ions, the binding constants in the presence of other ions were determined at 293 K under the experimental conditions. The results were listed in Table 5, showing that the binding constants between NCPAC and HSA decreased in the presence of most of the other ions. This indicated that the presence of other ions directly affected the binding between NCPAC and HSA. The competition between coexistent ions and NCPAC decreased the binding constant, which might shorten the storage time of the nucleotide drug in the blood plasma and weaken the maximum effectiveness.

Conclusions

In this work, an effective one-pot approach to NCPAC was developed. The interaction between NCPAC and HSA was studied by

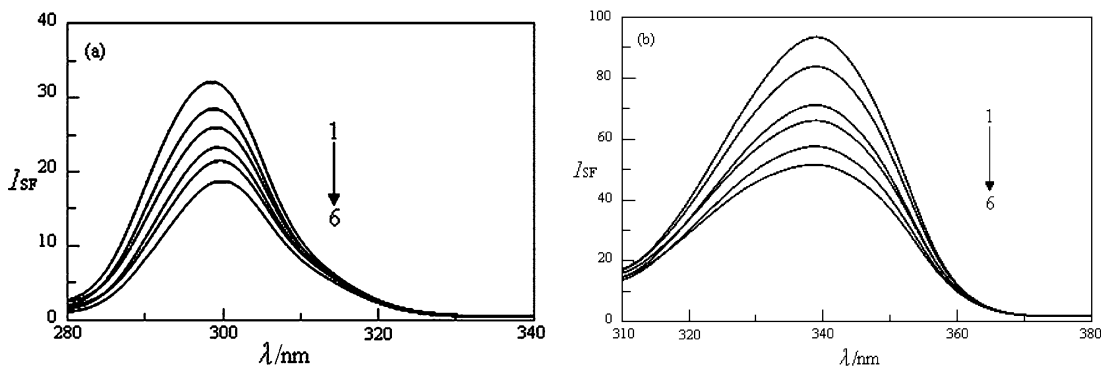

Fig. 10 The synchronous fluorescence spectra of HSA at NCPAC various concentrations while the $\Delta\lambda$ = 15 nm (a) and $\Delta\lambda$ = 60 nm (b). $C_{HSA} = 4.0 \times 10^{-7}$ mol L^{-1}, 1–6: $C_{NCPAC} = 0, 0.1, 0.2, 0.3, 0.4, 0.5 \times 10^{-6}$ mol L^{-1}.

Table 5 The binding constants between NCPAC and HSA at 300 K in the presence of common ions

Ions	$K(10^4)$	R_{HSA}	Ions	$K(10^4)$	R_{HSA}
K^+	1.720	0.9999	Zn^{2+}	0.7279	0.9995
Ca^{2+}	1.239	0.9993	Pb^{2+}	0.2570	0.9990
NH_4^+	2.404	0.9981	Mg^{2+}	0.0409	0.9988
Bi^{3+}	1.980	0.9996	Cu^{2+}	0.7282	0.9999
$C_2O_4^{2-}$	1.569	0.9999	NO_3^-	1.534	0.9998
Mn^{2+}	2.011	0.9983	CO_3^{2-}	0.8326	0.9999
Ni^{2+}	0.9147	0.9992	PO_4^{3-}	2.041	0.9995
SO_4^{2-}	0.5317	0.9992	Fe^{3+}	0.8981	0.9998
Cd^{2+}	0.7259	0.9989	Al^{3+}	1.819	0.9988
Hg^{2+}	1.173	0.9999	Co^{2+}	0.4878	0.9986

fluorescence spectroscopy combined with molecular docking and synchronous fluorescence spectrophotometric techniques under simulative physiological conditions for the first time. This study showed that the intrinsic fluorescence of HSA was quenched through a static quenching mechanism and NCPAC most likely bound to the hydrophobic pocket located in subdomain IIA. Experimental results also showed that the binding of NCPAC to HSA induced a conformational change of HSA, which was further proved by analyzing the synchronous fluorescence spectra. The binding force was mainly hydrophobic interaction, two other interactions, electrostatic attraction and hydrogen bonding were also involved in the binding process.

Acknowledgements

The authors gratefully acknowledge the Nature Science Foundation of China (Nos. 30970696, 20772024).

References

1 A. J. Cocuzza, D. R. Chidester, S. Culp, L. Fitzgerald and P. Gilligan, *Bioorg. Med. Chem. Lett.*, 1999, **9**, 1063.
2 C. Garcia-Echeverria, P. Taxler and D. B. Evans, *Med. Res. Rev.*, 2000, **20**, 28.
3 Z. P. Wang, S. H. Chang and T. J. Kang, *Spectrochim. Acta, Part A*, 2008, **70**, 313.
4 R. M. Izatt, K. Pawlak, J. S. Bradshaw and R. L. Bruening, *Chem. Rev.*, 1991, **91**, 1721.
5 L. Prodi, F. Bolletta, M. Montaldi, N. Zaccheroni, P. B. Savage, J. S. Bradshaw and R. M. Izatt, *Tetrahedron Lett.*, 1998, **39**, 5451.
6 H. M. Guo, J. Wu, H. Y. Niu, D. C. Wang, F. Zhang and G. R. Qu, *Bioorg. Med. Chem. Lett.*, 2010, **20**, 3098.
7 Y. J. Hu, Y. O. Yang, C. M. Dai, Y. Liu and X. H. Xiao, *Biomacromolecules*, 2010, **11**, 106.
8 K. K. Park, J. W. Park and A. D. Hamilton, *Org. Biomol. Chem.*, 2009, **7**, 4225.
9 P. Cohen, *Biochem. J.*, 2010, **425**, 53.
10 L. Trnková, I. Boušová, V. Staňková and J. Držata, *J. Mol. Struct.*, 2011, **985**, 243.
11 C. Xu, A. P. Zhang and W. P. Liu, *Pestic. Biochem. Physiol.*, 2007, **88**, 176.
12 Y. L. Wei, J. Q. Li, C. Dong, S. M. Shuang, D. S. Liu and C. W. Huie, *Talanta*, 2006, **70**, 377.
13 M. Rarey, B. Kramer, T. Lengauer and G. Klebe, *J. Mol. Biol.*, 1996, **261**, 470.
14 M. R. Eftink and C. A. Ghiron, *Biochemistry*, 1976, **15**, 672.
15 L. Trynda-Lemiesz, B. K. Keppler and H. Koztowski, *J. Inorg. Biochem.*, 1999, **73**, 123.
16 Z. X. Chi and R. T. Liu, *Biomacromolecules*, 2011, **12**, 203.
17 G. Z. Chen, X. Z. Huang, J. G. Xu, Z. Z. Zheng, Z. B. Wang, *Methods of fluorescence analysis*, Science Press, Beijing, 2nd edn, 1990.
18 J. Zhu, J. J. Li and J. W. Zhao, *Sens. Actuators, B*, 2009, **138**, 9.
19 P. Daneshgar, A. A. Moosavi-Movahedi, P. Norouzi, M. R. Ganjali, A. Madadkar-Sobhani and A. A. Saboury, *Int. J. Biol. Macromol.*, 2009, **45**, 129.
20 Y. Lu, Q. Q. Feng, F. L. Cui, W. W. Xing, G. S. Zhang and X. J. Yao, *Bioorg. Med. Chem. Lett.*, 2010, **12**, 469.
21 Q. Wang, Y. H. Zhang, H. J. Sun, H. L. Chen and X. G. Chen, *J. Lumin.*, 2011, **131**, 206.
22 C. Q. Jiang, M. X. Gao and X. Z. Meng, *Spectrochim. Acta, Part A*, 2003, **59**, 1605.
23 N. Juziro and M. Noriko, *Chem. Pharm. Bull.*, 1985, **33**, 2522.
24 P. D. Ross and S. Subramanian, *Biochemistry*, 1981, **20**, 3096.
25 T. Förster, *Modern Quantum Chemistry 3*, Sinanoglu, Academic Press, New York, 1996.
26 T. K. Maiti, K. S. Ghosh, A. Samanta and S. Dasgupta, *J. Photochem. Photobiol., A*, 2008, **194**, 297.
27 C. W. Wu and L. Stryer, Proximity relationships in rhodopsin, *Proc. Natl. Acad. Sci. U. S. A.*, 1972, **69**, 1104.
28 J. R. Lakowicz, *Principles of fluorescence spectroscopy*, Plenum Press, New York, 1983.
29 F. L. Cui, Y. R. Cui, H. X. Luo, X. J. Yao, J. Fan and Y. Lu, *Chin. Sci. Bull.*, 2006, **51**, 2201.
30 T. Peters, *Biochemistry, Genetics and Medical Applications*, Academic Press, San Diego, CA, 1996.
31 F. L. Cui, Y. H. Yan, Q. Z. Zhang, J. Du, X. J. Yao, G. R. Qu and Y. Lu, *Polish J. Chem.*, 2009, **83**, 1783.
32 J. N. Miller, *Proc. Anal. Div. Chem. Soc.*, 1979, **16**, 203.
33 A. Varlan and M. Hillebrand, *Molecules*, 2010, **15**, 3905.
34 P. N. Naik, S. A. Chimatadar and S. T. Nandibewoor, *J. Photochem. Photobiol., B*, 2010, **100**, 147.
35 H. Liang, J. Huang, C. Q. Tu, M. Zhang, Y. Q. Zhou and P. W. Shen, *J. Inorg. Biochem.*, 2001, **85**, 167.